



Research paper

Paper-based aqueous Al ion battery with water-in-salt electrolyte

Yifei Wang^{a,b,*}, Wending Pan^b, Kee Wah Leong^b, Yingguang Zhang^b, Xiaolong Zhao^b,
Shijing Luo^b, Dennis Y.C. Leung^{b,*}^a School of Mechanical Engineering and Automation, Harbin Institute of Technology, Shenzhen, China^b Department of Mechanical Engineering, The University of Hong Kong, Hong Kong, China

Received 12 August 2021; revised 6 October 2021; accepted 12 October 2021

Available online ■■■

Abstract

Low-cost, flexible and safe battery technology is the key to the widespread usage of wearable electronics, among which the aqueous Al ion battery with water-in-salt electrolyte is a promising candidate. In this work, a flexible aqueous Al ion battery is developed using cellulose paper as substrate. The water-in-salt electrolyte is stored inside the paper, while the electrodes are either printed or attached on the paper surface, leading to a lightweight and thin-film battery prototype. Currently, this battery can tolerate a charge and discharge rate as high as 4 A g^{-1} without losing its storage capacity. The charge voltage is around 2.2 V, while the discharge plateau of 1.6–1.8 V is among the highest in reported aqueous Al ion batteries, together with a high discharge specific capacity of $\sim 140 \text{ mA h g}^{-1}$. However, due to the water electrolysis side reaction, the faradaic efficiency can only reach 85% with a cycle life of 250 due to the dry out of electrolyte. Benefited from using flexible materials and aqueous electrolyte, this paper-based Al ion battery can tolerate various deformations such as bending, rolling and even puncturing without losing its performance. When two single cells are connected in series, the battery pack can provide a charge voltage of 4.3 V and a discharge plateau as high as 3–3.6 V, which are very close to commercial Li ion batteries. Such a cheap, flexible and safe battery technology may be widely applied in low-cost and large-quantity applications, such as RFID tags, smart packages and wearable biosensors in the future.

© 2021, Institute of Process Engineering, Chinese Academy of Sciences. Publishing services by Elsevier B.V. on behalf of KeAi Communications Co., Ltd. This is an open access article under the CC BY-NC-ND license (<http://creativecommons.org/licenses/by-nc-nd/4.0/>).

Keywords: Al ion battery; Aqueous electrolyte; Water-in-salt; Paper battery; Flexible battery

1. Introduction

With the widespread usage of portable electronics, low-cost and environmentally-friendly energy storage units are in urgent demand. Currently, Li ion battery is the mainstream and the most mature battery technology for this mission, which is, however, restricted by several issues such as high fabrication cost, limited metal resources, battery disposal pollution and safety hazards. Regarding this, the research and development of various non-Li ion battery technologies are getting more

and more popular in recent years, including the K ion [1], Na ion [2], Zn ion [3], Mg ion [4] and Al ion batteries [5].

The selection of electrolyte is of key importance to all metal ion batteries. Compared with organic electrolyte, the aqueous electrolyte is favorable for its low price, high conductivity and better safety without combustion or explosion concerns [6]. Nevertheless, not all the metal ion batteries can use aqueous electrolyte because of both the metal-water reaction during battery standby and the water electrolysis side reaction during battery recharge. In general, the more active of the metal electrode, the less feasible of using aqueous electrolyte. Among them, the Zn metal is currently the most suitable choice because of its higher reduction potential (-0.76 V vs SHE) than that of H_2 evolution (-0.83 V vs SHE), leading to a vast study on aqueous Zn ion batteries [3].

* Corresponding authors.

E-mail addresses: yifeiwang@hit.edu.cn (Y. Wang), ycleung@hku.hk (D.Y.C. Leung).

<https://doi.org/10.1016/j.gee.2021.10.001>

2468-0257/© 2021, Institute of Process Engineering, Chinese Academy of Sciences. Publishing services by Elsevier B.V. on behalf of KeAi Communications Co., Ltd. This is an open access article under the CC BY-NC-ND license (<http://creativecommons.org/licenses/by-nc-nd/4.0/>).

Please cite this article as: Y. Wang et al., Paper-based aqueous Al ion battery with water-in-salt electrolyte, Green Energy & Environment, <https://doi.org/10.1016/j.gee.2021.10.001>

Alternatively, the Al metal is also feasible for developing aqueous Al ion batteries in spite of its lower reduction potential (-1.66 V vs SHE). Compared with Zn, Al is favorable because of its greater abundance in the earth crust (8.3%). In addition, Al has a three-electron redox reaction mechanism, which can store more energy than other metals. The specific capacity of Al is as high as 2980 mA h g^{-1} , which is 3.6 times of Zn. As for the volumetric capacity, Al also has a 37% higher value of 8046 mA h cm^{-3} [7]. Therefore, many researchers have engaged in the development of aqueous Al ion battery in recent decade. In the early stage of development, diluted Al salt solution was used as electrolyte directly, including $AlCl_3$ [8–10], $Al_2(SO_4)_3$ [11–13], $Al(NO_3)_3$ [14,15], $Al(CF_3SO_3)_3$ [16], etc. Many electrode materials with high Al^{3+} storage capacity were developed, such as TiO_2 [17–20], $CuHCF$ [11,21], V_2O_5 [10], Graphite [14,22,23] and MoO_3 [24–26]. However, full battery testing was difficult in this system when using Al foil as negative electrode due to the significant H_2 evolution side reaction. Alternatively, non-Al materials were used for both positive and negative electrodes to avoid this issue, but the specific capacity would be significantly reduced [14,21,23]. To tackle this problem, recently, the aluminum trifluoromethanesulfonate ($Al(OTf)_3$) electrolyte was employed for aqueous Al ion battery, which achieved much higher specific capacity when using Al as negative electrode [27–32]. However, the price of $Al(OTf)_3$ is even higher than the ionic electrolyte (e.g. $AlCl_3/[EMIm]Cl$), which greatly hampers its wide application [33]. To control the cost, a super-concentrated $AlCl_3$ solution, namely the water-in-salt electrolyte, has been tried for developing an aqueous Al ion battery, which was found to lower down the H_2 evolution potential to -2.3 V vs SHE [33]. In this manner, the side reaction is greatly suppressed, ensuring a normal battery recharge when using Al as negative electrode.

Recently, flexible electronics such as various wearable sensors are also under rapid development, calling for the research on low-cost and highly-safe flexible power sources [34]. These flexible power sources will undergo frequent deformations such as bending, rolling and even extreme situations such as puncturing, which bring much harsher requirement on their safety level. To avoid potential electrolyte leakage, gel electrolytes based on PVA, gelatin or PAM have been developed for aqueous Al ion batteries in literature [35–37]. Furthermore, the water-in-salt aqueous Al ion battery is also very suitable for this mission, as long as the semi-solid electrolyte can be well stored in a thin-film pattern. To achieve this goal, cellulose paper can be a suitable substrate for the electrolyte storage [38], which can firstly absorb the diluted electrolyte solution by capillary action, and then convert to the water-in-salt electrolyte by water removal via a baking process. The electrodes can also be printed onto the paper surface conveniently, leading to a thin-film and lightweight battery technology, which has never been reported to the best of our knowledge.

In this work, a paper-based aqueous Al ion battery was developed for the first time, which stored a water-in-salt (i.e. $AlCl_3$) inside a paper as electrolyte. Low-cost materials such

as a piece of 99.9% pure Al foil was employed as the negative electrode while the positive electrode can be printed on the paper with a graphite ink, and the whole battery was encapsulated in a plastic thin-film. The battery performance was evaluated at room temperature by different electrochemical techniques, and the battery electrodes were characterized by SEM, EDX and XPS. In addition, the battery's flexibility was examined under different types of deformation, such as bending, rolling and puncturing. Furthermore, a two-cell battery pack was developed successfully to accommodate the voltage output to commercial Li ion batteries. Finally, a new cell structure was proposed in order to further improve the cycling stability.

2. Experimental

2.1. Materials

Low-cost materials were used for fabricating the current paper-based Al ion battery. Filter paper (Whatman™) was used as battery substrate, 99.9% pure Al foil (0.1 mm thick, Aladdin®) was selected as negative electrode without any surface treatment, and $AlCl_3 \cdot 6H_2O$ (Aladdin®) was utilized for the preparation of electrolyte. As for the positive electrode, graphite powder (325 mesh, Aladdin®), acetylene black, polyvinylidene fluoride binder (PVDF, Sigma–Aldrich) and absolute ethanol solvent (BDH®) were employed to prepare a graphite ink, while a commercial carbon ink (CH-8, JELCON) was used for printing the current collector. Finally, the whole cell assembly was packaged by plastic thin-film from a local stationary shop. All materials were used as received without any further treatment.

2.2. Battery design and fabrication

Fig. 1 exhibits both the cross-sectional view and the exploded view of the paper-based Al ion battery. First, a graphite ink was prepared by dispersing 20 mg graphite powder, 2.5 mg PVDF and 2.5 mg acetylene black into 1 mL ethanol–water solvent (1:1), which was sonicated for 30 min to achieve satisfactory uniformity. Next, 20 μ L of the as-prepared ink was deposited onto the filter paper by a pipette and dried. To collect the current from the graphite electrode, an extra carbon ink was screen printed onto the graphite ink, both covering it and connecting it to the Cu end. After drying at 60 °C for 1 h and subsequently hot-pressed at 90 °C and 1 MPa for 5 min, the positive electrode was completed. For preparation of the water-in-salt electrolyte, 100 μ L of the saturated $AlCl_3$ solution was dropped onto the filter paper and absorbed uniformly. Afterwards, it was baked at 60 °C for 30 min in order to remove the excess water, so that a highly-concentrated form of $AlCl_3$ could be obtained. Finally, the Al foil was attached directly onto the other side of paper, and the assembled battery was well sealed in a plastic film with its fringes hot-pressed. Both electrodes had an active area of 1 cm \times 1 cm, and the weight of deposited graphite (0.4 mg) was used to calculate the specific current, capacity and energy.

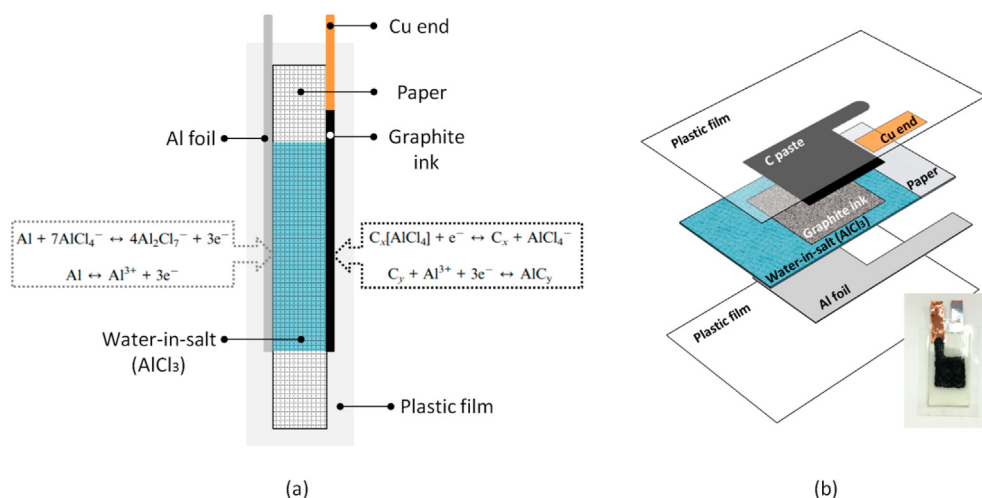


Fig. 1. Design and fabrication of the paper-based aqueous Al ion battery: (a) Battery cross-sectional view and detailed working principle; (b) Exploded view of the battery structure (inset: real lab prototype).

The as-fabricated paper-based Al ion battery had a total weight of 0.3 g only, while the estimated cost was about 0.002 USD/cell.

According to our previous study on the water-in-salt Al ion battery [33], the detailed reactions at the two electrodes are also specified in Fig. 1a. In general, three types of Al ions co-exist in the water-in-salt AlCl_3 electrolyte, namely the Al^{3+} , AlCl_4^- and Al_2Cl_7^- , whose composition varies along with the battery cycling process. For the Al negative electrode, the dissolution and deposition of Al occur repetitively; while for the graphite positive electrode, both Al^{3+} and AlCl_4^- can be intercalated into and de-intercalated from the carbon layers of graphite during charging/discharging. Moreover, water electrolysis side reaction may also happen during battery charging due to the presence of water, but its extent is greatly reduced due to the limited amount of water in the water-in-salt electrolyte.

2.3. Battery test and characterization

After assembly, open circuit voltage (OCV) of the battery was firstly measured, which was about 0.7 V. This low OCV could be related to the parasitic Al-air reaction with salt electrolyte, which should be originated from the dissolved oxygen inside the aqueous electrolyte. However, the battery voltage would quickly drop to zero when it was discharged, due to the very limited amount of oxygen inside. Next, the battery was charged and discharged at different specific currents (0.25–4.00 A/g) for multiple cycles using a battery testing workstation (LAND CT3001A), until the charging voltage reached upper limit of the workstation (i.e. 5 V) and triggered the end of testing. For the charging process, the charge time was controlled according to the theoretical capacity of graphite for Al ion intercalation ($\sim 165 \text{ mAh g}^{-1}$ [33]); while for the discharging process, a limiting voltage of 0.8 V was set in order to avoid the parasitic Al-air reaction. The stabilized battery performance after 100 cycles was used to compare the effect of different specific currents. In addition

to the cycle test, a rate test was also conducted by charging the battery at 1 A g^{-1} consistently, while discharging it at different specific currents from 0.25 to 4 A g^{-1} . Furthermore, a CV test was conducted by scanning the battery between 0 and 3.5 V with a scan rate of 50 mV s^{-1} .

To characterize the paper-based water-in-salt electrolyte and the Al negative electrode before and after battery cycling (100 cycles at 1 A g^{-1}), scanning electron microscopy (SEM, Hitachi S3400) and energy dispersive X-ray detector (EDX) were employed. As for the positive electrode, a special battery design was utilized by using carbon paper-supported graphite instead of printed graphite. In this manner, the graphite positive electrode could also be detached and fully rinsed for further characterization, which could represent the printed graphite electrode on the filter paper. First, X-ray photoelectron spectroscopy (XPS) was adopted to study the bonding status of different elements (C, Al, Cl) inside the graphite electrode. Next, surface morphology of the electrodes was compared before and after the cycle test using SEM, and the elemental composition was also investigated by EDX.

3. Results & discussion

3.1. Electrolyte characterization

Before battery testing, the water-in-salt AlCl_3 electrolyte in the paper substrate was characterized first by SEM and EDX. As shown in Fig. 2a, the electrolyte surface had a dense and flat structure with water-in-salt AlCl_3 filling in all the space among cellulose fibers, which was very different from the pristine paper surface in the inset. Fig. 2b exhibits the element mapping result of a selected area on the electrolyte surface. Four major elements were identified, including C from the cellulose fiber, Al and Cl from the AlCl_3 , and O from both the cellulose fiber and water, as shown in Fig. 2c–f. Apparently, the C element mainly located in the fiber area, while the Al and Cl element mainly located in the water-in-salt electrolyte area. As for the O element, it could be observed in both areas.

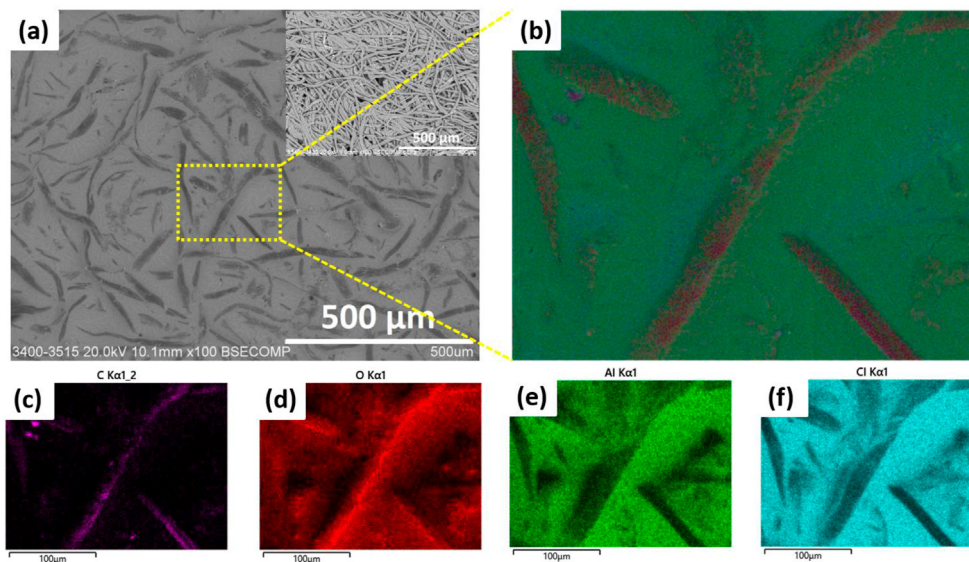


Fig. 2. Characterization of the water-in-salt AlCl_3 electrolyte in the paper substrate: (a) SEM image of its surface morphology; (b) Element mapping of a selected area, including (c) C; (d) O; (e) Al and (f) Cl.

From our previous study on the water-in-salt AlCl_3 electrolyte, both Al_2Cl_7^- and AlCl_4^- ions exist in the electrolyte in addition to Al^{3+} , of which the AlCl_4^- ion was reported to be of key importance to the high discharge voltage plateau at around 1.8 V [33].

3.2. Battery performance

According to our previous study, the maximum specific capacity of graphite for Al ion intercalation was about 165 mA h g^{-1} [33]. Therefore, in this work, the charging capacity was controlled to be 165 mA h g^{-1} , leading to different charging times for different specific currents (that is, 40 min for 0.25 A g^{-1} , 20 min for 0.5 A g^{-1} , 10 min for 1 A g^{-1} , etc.). As shown in Fig. 3a, the paper-based Al ion battery exhibited a discharge plateau of 1.6–1.8 V, which was quite high compared with other aqueous Al ion batteries in literature [39]. With a cut-off voltage of 0.8 V, the discharge specific capacity of $\sim 140 \text{ mA h g}^{-1}$ was less than 165 mA h g^{-1} , indicating that part of the energy input during charging was wasted due to other side reactions, such as water electrolysis. As for the charging voltage, the value was around

2.0–2.2 V when lower specific currents were selected, which would however rise to above 3 V when the specific current exceeded 1 A g^{-1} . This was probably due to the higher resistance of the paper-based water-in-salt electrolyte, which could not tolerate a too high charging rate. Therefore, a moderate value of 1 A g^{-1} (6C) was optimal for this battery, which could achieve a fine balance between charging time and energy efficiency. Moreover, Fig. 3b shows the rate test of the battery, which was constantly charged at 1 A g^{-1} and discharged at different rates continuously. Apparently, the paper-based Al ion battery could undertake different discharge rates without losing the capacity evidently, and the coulombic efficiency was around 80%. At lower discharge rates such as 0.25 A g^{-1} , the specific capacity was slightly lower, which was consistent with the result in Fig. 3a. The loss of coulombic efficiency would probably be related to the water electrolysis side reaction during battery charging, which was originated from the remaining water inside the water-in-salt electrolyte.

During the cycle test, a battery activation process was noticed for each new battery, which generally took about 100 cycles before the discharge specific capacity reached its maximum value. This phenomenon was also observed in the

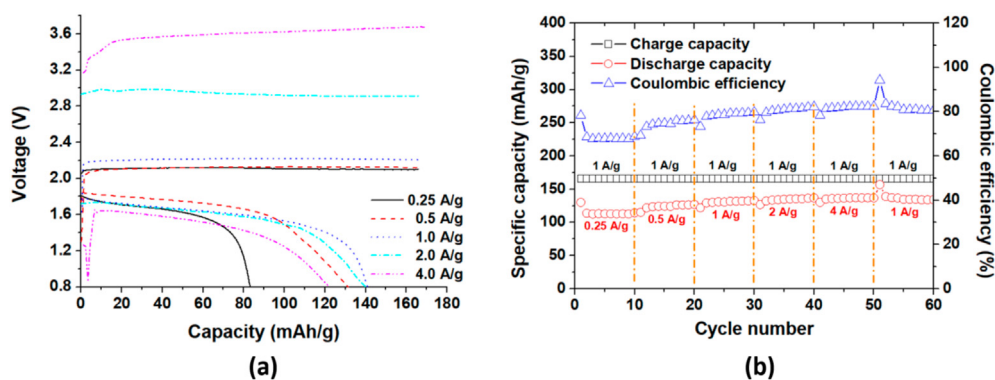


Fig. 3. Battery performance at different specific currents: (a) Charge and discharge curves at $0.25\text{--}4.0 \text{ A g}^{-1}$; (b) Rate test with a constant charge rate of 1 A g^{-1} and various discharge rates of 0.25, 0.5, 1, 2 and 4 A g^{-1} .

CV scan as shown in Fig. 4a. With more and more scanning cycles, both the charge and discharge peaks increased, indicating that the battery was gradually activated by the cycling process. Fig. 4b gives a more direct proof of the battery activation process. The battery was cycled at 1 A g^{-1} continuously until the charging voltage increased to 5 V, which is the voltage upper limit of the workstation so that the testing would be stopped. At the first 25 cycles, both the discharge capacity and the coulombic efficiency increased dramatically. Afterwards, the values kept increasing until reaching a steady state at cycle-100, which were maintained for another 150 cycles until battery failure. Therefore, the current paper-based Al ion battery could survive for 250 cycles in total. The increment of charging voltage at the final stage should be related to the loss of water via the water electrolysis side reaction, which led to an elevation of the battery ionic resistance. To prove this, the detached paper-based AlCl_3 electrolyte from a failed battery was investigated by SEM and compared with its pristine state. As shown in Fig. 4c, the cellulose fiber network once underneath the water-in-salt AlCl_3 was fully exposed, together with hollow space observed. Also, some crystalline AlCl_3 flakes were observed on the cellulose fiber (Fig. 4d), indicating that the electrolysis of water further dried the water-in-salt electrolyte and caused the battery failure.

3.3. Electrode characterization

In order to conduct post-test characterization of the graphite electrode, a special battery design was used in which the graphite was coated on an independent carbon paper instead of

on the paper substrate directly. In this manner, the graphite electrode could be detached from the battery after cycling, which was sonicated and fully rinsed by DI water before carrying out the XPS analysis. Fig. 5 shows the chemical state of different elements in the graphite after battery cycling, including C, O, Al and Cl. As shown in Fig. 5b, in addition to the sp^2 main peak at 284.8 eV representing the pristine graphite, a sp^3 peak at 285.6 eV and a C–O peak at 286.4 eV were also observed for the C element, indicating the possible electrochemical oxidation of the graphite by the intercalation of aluminum and chloroaluminate ions [40]. Fig. 5c,d further prove the existence of aluminum and chloroaluminate ions inside the used graphite. Specifically, for the Cl element, in addition to the two peaks at 198.9 and 200.0 eV representing the chloride Cl, another two peaks at 200.8 and 201.8 eV represent the organic Cl, which should be the C–Cl bond formed during ion intercalation [33]. To sum up, the XPS results prove the intercalation of Al- and Cl-containing ions during the battery cycle test, including both Al^{3+} and AlCl_4^- .

Surface morphology of the Al negative electrode and graphite positive electrode before and after the cycle test was also compared. As shown in Fig. 6a,b, the flat surface of the pristine Al foil was partially corroded by the water electrolysis side reaction, leading to a bumpy surface with multiple micro holes. From this point of view, the present paper-based Al ion battery is imperfect compared with its organic electrolyte-based counterparts. However, considering its low fabrication cost and high safety level, it is still promising for some specific applications with large production quantity and less cycle durability requirement, such as RFID tags, smart packages and wearable biosensors. As for the positive electrode (Fig. 6c,d),

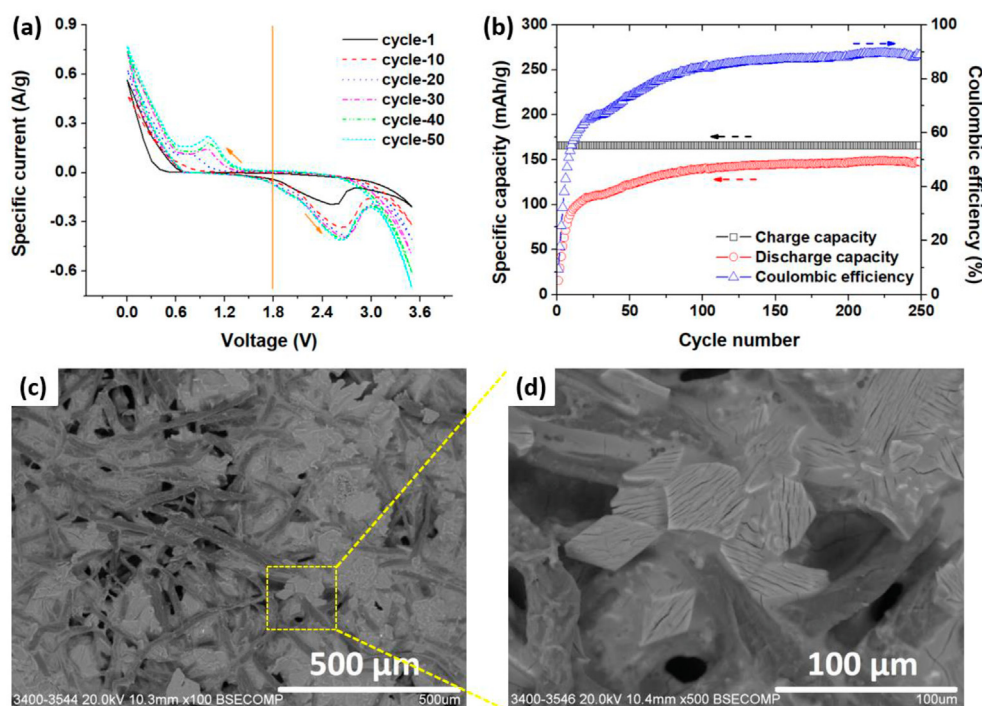


Fig. 4. Battery activation and cycle stability: (a) CV curves of a new battery between 0–3.5 V; (b) Cycle stability of a new battery at 1 A g^{-1} , together with the variation of coulombic efficiency; (c) SEM image of the paper-based water-in-salt electrolyte after cycle test; (d) Higher magnification of the crystalline AlCl_3 residue.

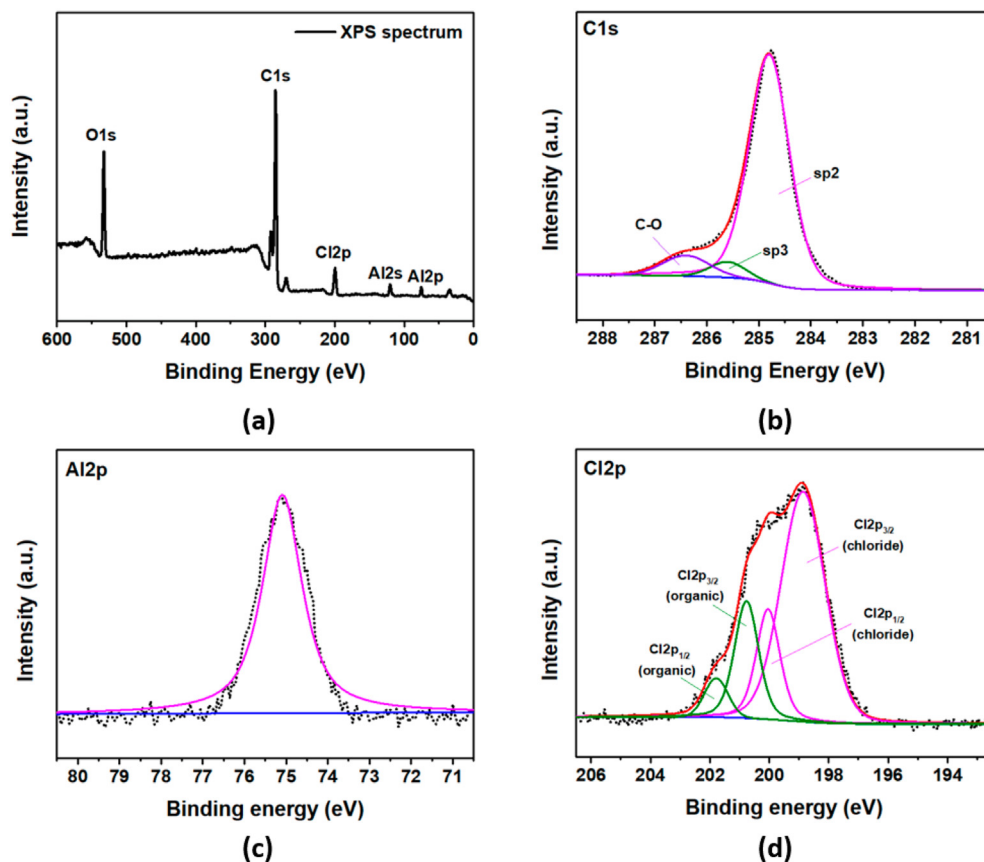


Fig. 5. XPS analysis of the graphite electrode after 100 cycles at 1 A g^{-1} : (a) Survey spectrum; (b) high resolution C 1s; (c) high resolution Al 2p; (d) high resolution Cl 2p.

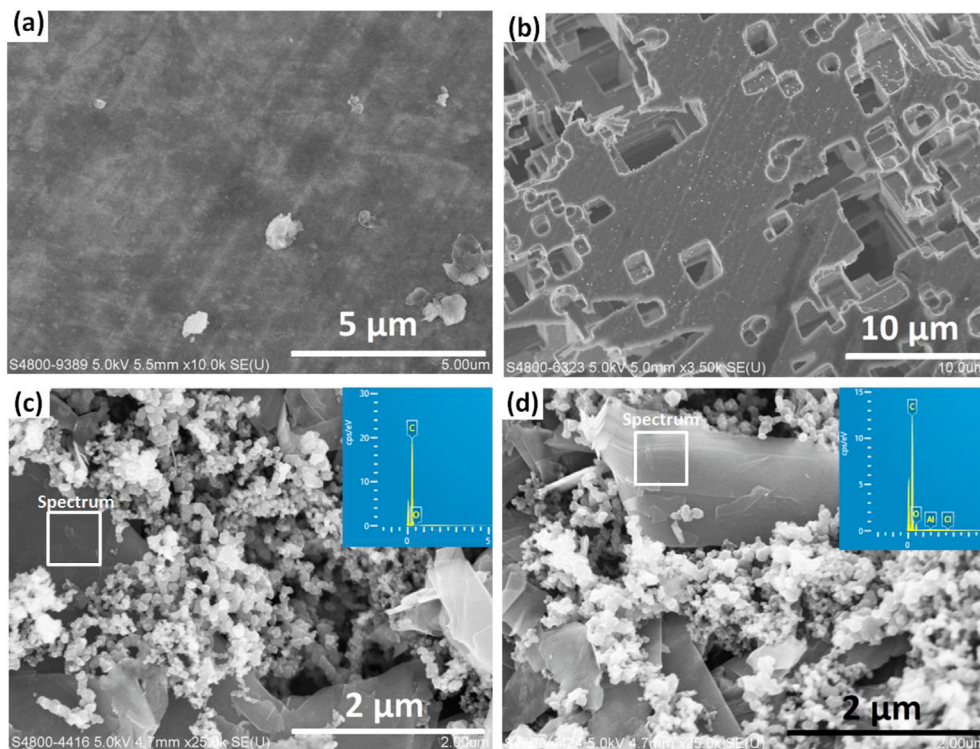


Fig. 6. SEM images of the Al and graphite electrodes before and after the cycle test: (a) Al electrode before cycle; (b) Al electrode after cycle; (c) Graphite electrode before cycle (inset: EDX result); (d) Graphite electrode after cycle (inset: EDX result).

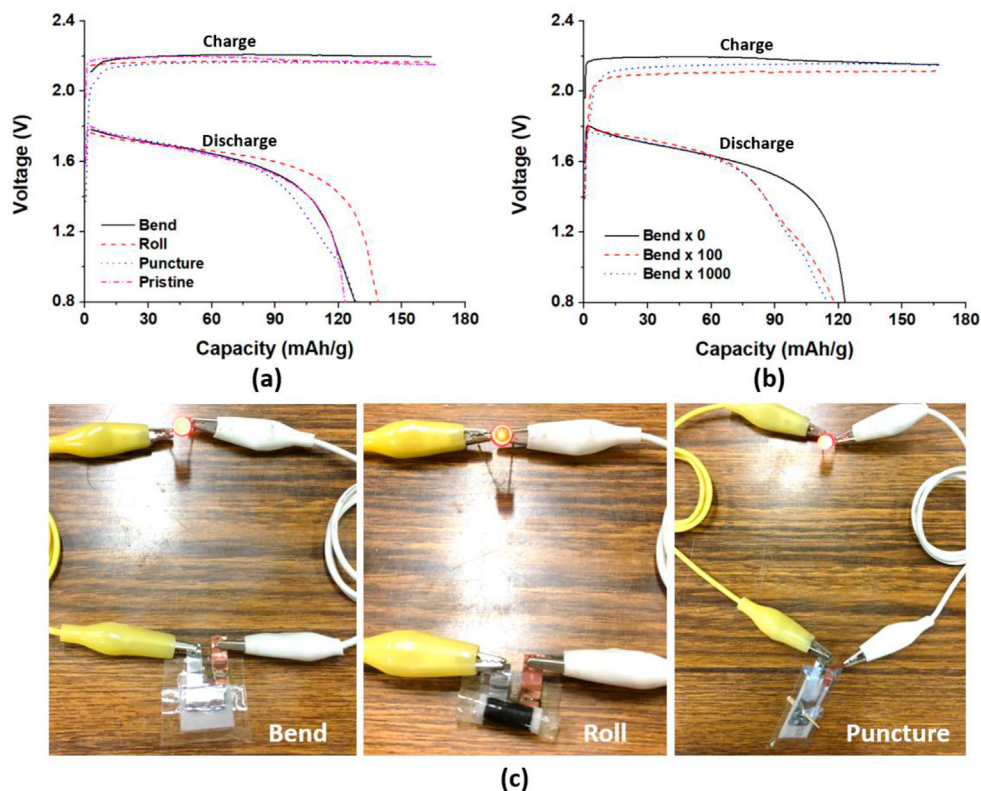


Fig. 7. Flexibility study of the paper-based Al ion battery: (a) Battery performance at 1 A g^{-1} under different types of deformation; (b) Battery performance at 1 A g^{-1} after different bending times; (c) Demonstration of a LED light powered by deformed batteries.

the large graphite flakes connected by acetylene black micro particles were not changed evidently, proving its high structural stability. Also, the major element for the pristine graphite was C and O, while extra element of Al and Cl were detected in the cycled graphite (from the inset of EDX result), proving the intercalation of aluminum and chloroaluminate ions during battery cycling. In conclusion, the Al and graphite electrodes were not the reason behind the poor cycle durability, while water loss of the electrolyte should be the major issue for the current paper-based Al ion battery.

3.4. Battery flexibility study

By using filter paper as substrate and water-in-salt AlCl_3 stored inside as electrolyte, the current paper-based Al ion battery is intrinsically flexible and highly safe against various deformations, which is especially promising for powering various flexible and wearable electronic devices. As shown in Fig. 7a, when the battery was bended, rolled or even punctured by a needle, the charge–discharge performance was not varied evidently. The charging voltage was kept around 2.2 V, while the discharge plateau was maintained between 1.6 and 1.8 V together with a discharge specific capacity of 120–140 mA h g^{-1} . Moreover, the battery performance was proved to be quite robust against multiple bending times as shown in Fig. 7b, proving its high application potential in dynamic environments such as body sensors. Furthermore, Fig. 7c demonstrates a LED light powered by the paper-based Al ion battery at different deformation status, exhibiting its excellent flexibility and safety level in real applications.

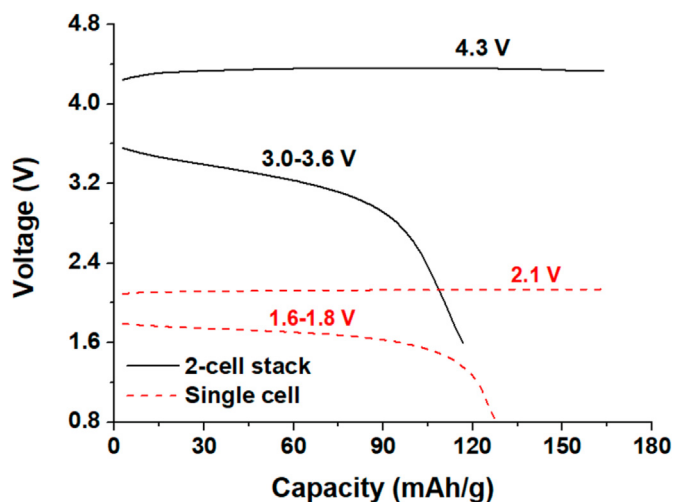


Fig. 8. Comparison between a paper-based Al ion single battery and a 2-cell battery pack.

3.5. Battery stacking

Currently, the portable electronic market is dominated by Li ion batteries, which generally provide a charge voltage of 3.6–4.2 V and a discharge voltage of 3.2–3.7 V. To accommodate this mature market, the current paper-based Al ion battery should be stacked in series in order to meet the voltage requirement. As shown in Fig. 8, a 2-cell battery pack connected in series could provide a charging voltage around 4.3 V

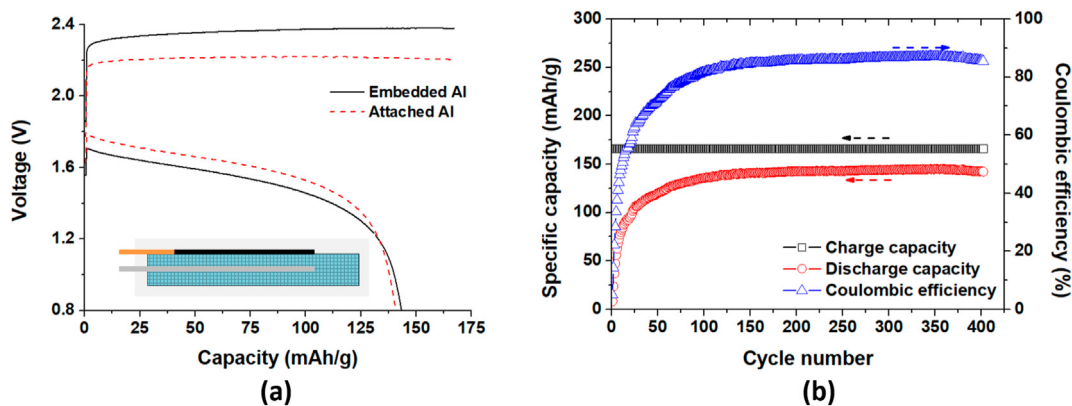


Fig. 9. New battery structure with embedded Al foil inside paper: (a) Comparison of battery performance between the cell with attached Al foil and embedded Al foil; (b) Improved cycle stability of the latter case.

and a discharge plateau of 3.0–3.6 V, which were very close to the values of Li ion batteries. As for the discharge capacity, a slight decrease of 9% was observed for the 2-cell battery pack when the cut-off voltage was set as 1.6 V, which could be attributed to the performance difference between the single cells as well as the extra ohmic loss from the connection part. In conclusion, we believe that this paper-based Al ion battery pack is promising for substituting some of the Li ion batteries in flexible electronic devices, especially for those with low cost, large quantity and less cycling requirement, such as RFID tags, smart packages and wearable sensors [41–43].

3.6. New battery structure

To improve the contact between the Al foil and the paper-based water-in-salt electrolyte, an electrode embedding design was further studied by storing the Al foil inside the paper substrate during the paper making process [44]. Afterwards, the graphite ink and carbon paste were printed onto the paper surface as positive electrode. The as-prepared device was subsequently immersed in saturated AlCl_3 solution to allow sufficient electrolyte uptake, which was next baked at 60 °C for 30 min to obtain the water-in-salt electrolyte. Fig. 9a compares the performance between batteries with either the previous attached Al electrode and the present embedded Al electrode. The latter case obtained slightly higher charging voltage and lower discharge plateau, which should be correlated to the higher thickness of home-made paper with an increased ohmic resistance. Nevertheless, the battery cycling stability could be significantly improved by this new battery structure. As shown in Fig. 9b, the cycle number was increased from 250 to 400, which was mainly attributed to the higher electrolyte storage capacity of the new battery structure. In the future, other strategies will also be investigated to improve the battery durability, such as passive water uptake from the ambient, or gelling the water-in-salt electrolyte.

4. Conclusions

In this work, a paper-based aqueous Al ion battery was developed for the first time by storing a water-in-salt AlCl_3 electrolyte inside a paper substrate. The battery consists of a graphite

electrode which was directly printed onto the paper surface, and an Al foil electrode which was either attached on the paper or embedded inside it. This low-cost and green battery technology could provide a voltage output of 1.6–1.8 V and a specific capacity of $\sim 140 \text{ mA h g}^{-1}$ at 1 A g^{-1} , which were among the highest in reported aqueous Al ion batteries. The production cost was as low as 0.002 USD/cell, leading to 2.8 USD/W and 35.7 USD/Ah, respectively. The charge–discharge faradaic efficiency was around 85% due to the water electrolysis side reaction, which was also the major reason behind its limited cycle lifetime (250 cycles). Nevertheless, this value could be improved to 400 cycles if more electrolyte was stored inside the paper. The current paper-based Al ion battery was also robust against various deformations such as bending, rolling and puncturing, which could maintain its performance without burning or explosion hazards. When two cells were connected in series, a working voltage close to commercial Li ion batteries could be obtained. Such a low-cost, high-safety and environmentally-friendly battery technology is a promising candidate for powering large-quantity RFID tags, smart packages and wearable biosensors in the near future.

Conflict of interest

The authors declare that they have no known competing financial interests or personal relationships that could have appeared to influence the work reported in this paper.

Acknowledgement

The authors would like to acknowledge the CRF grant of the Hong Kong Research Grant Council (C5031-20G), the CRCG grant of the University of Hong Kong (201910160008) and the research start-up fund of Harbin Institute of Technology, Shenzhen (CA45001039) for providing funding support to this project.

References

- [1] T. Hosaka, K. Kubota, A.S. Hameed, S. Komaba, *Chem. Rev.* (2020).
- [2] T. Perveen, M. Siddiq, N. Shahzad, R. Ihsan, A. Ahmad, M.I. Shahzad, *Renew. Sustain. Energy Rev.* 119 (2020) 109549.
- [3] G. Fang, J. Zhou, A. Pan, S. Liang, *ACS Energy Lett.* 3 (2018) 2480–2501.

- [4] Z. Ma, D.R. Macfarlane, M. Kar, Batter. Supercaps 2 (2019) 115–127.
- [5] S.K. Das, S. Mahapatra, H. Lahan, J. Mater. ChemA. 5 (2017) 6347–6367.
- [6] F. Beck, P. Rüetschi, Electrochim. Acta 45 (2000) 2467–2482.
- [7] Y. Wang, H. Kwok, W. Pan, H. Zhang, D.Y. Leung, J. Power Sources 414 (2019) 278–282.
- [8] S. Liu, J. Hu, N. Yan, G. Pan, G. Li, X. Gao, Energy Environ. Sci. 5 (2012) 9743–9746.
- [9] Y. Liu, S. Sang, Q. Wu, Z. Lu, K. Liu, H. Liu, Electrochim. Acta 143 (2014) 340–346.
- [10] J. González, F. Nacimiento, M. Cabello, R. Alcántara, P. Lavela, J. Tirado, RSC Adv. 6 (2016) 62157–62164.
- [11] S. Liu, G. Pan, G. Li, X. Gao, J. Mater. ChemA. 3 (2015) 959–962.
- [12] B. Jin, S. Hejazi, H. Chu, G. Cha, M. Altomare, M. Yang, P. Schmuki, Nanoscale 13 (2021) 6087–6095.
- [13] L. Yan, X. Zeng, S. Zhao, W. Jiang, Z. Li, X. Gao, T. Liu, Z. Ji, T. Ma, M. Ling, ACS Appl. Mater. Interfaces 13 (2021) 8353–8360.
- [14] J. Joseph, J. Nerkar, C. Tang, A. Du, A.P. O'mullane, K.K. Ostrikov, ChemSusChem 12 (2019) 3753–3760.
- [15] Y. Ru, S. Zheng, H. Xue, H. Pang, Chem. Eng. J. 382 (2020) 122853.
- [16] Q. Pang, S. Yang, X. Yu, W. He, S. Zhang, Y. Tian, M. Xing, Y. Fu, X. Luo, J. Alloys Compd. 885 (2021) 161008.
- [17] S. Sang, Y. Liu, W. Zhong, K. Liu, H. Liu, Q. Wu, Electrochim. Acta 187 (2016) 92–97.
- [18] M. Kazazi, P. Abdollahi, M. Mirzaei-Moghadam, Solid State Ionics 300 (2017) 32–37.
- [19] H. Lahan, R. Boruah, A. Hazarika, S.K. Das, J. Phys. Chem. C 121 (2017) 26241–26249.
- [20] M. Ojeda, B. Chen, D.Y. Leung, J. Xuan, H. Wang, Energy Procedia 105 (2017) 3997–4002.
- [21] A. Holland, R. Mckerracher, A. Cruden, R. Wills, J. Appl. Electrochem. 48 (2018) 243–250.
- [22] S. Nandi, S.K. Das, ACS Sustain. Chem. Eng. 7 (2019) 19839–19847.
- [23] S. Nandi, H. Lahan, S.K. Das, Bull. Mater. Sci. 43 (2020) 1–7.
- [24] J. Joseph, A.P. O'mullane, K. Ostrikov, ChemElectroChem 6 (2019) 6002–6008.
- [25] H. Lahan, S.K. Das, J. Power Sources 413 (2019) 134–138.
- [26] H. Lahan, S.K. Das, Ionics 25 (2019) 3493–3498.
- [27] S. He, J. Wang, X. Zhang, J. Chen, Z. Wang, T. Yang, Z. Liu, Y. Liang, B. Wang, S. Liu, Adv. Funct. Mater. 29 (2019) 1905228.
- [28] C. Wu, S. Gu, Q. Zhang, Y. Bai, M. Li, Y. Yuan, H. Wang, X. Liu, Y. Yuan, N. Zhu, Nat. Commun. 10 (2019) 1–10.
- [29] Y. Cai, S. Kumar, R. Chua, V. Verma, D. Yuan, Z. Kou, H. Ren, H. Arora, M. Srinivasan, J. Mater. ChemA. 8 (2020) 12716–12722.
- [30] Y. Gao, H. Yang, X. Wang, Y. Bai, N. Zhu, S. Guo, L. Suo, H. Li, H. Xu, C. Wu, ChemSusChem 13 (2020) 732–740.
- [31] S. Kumar, V. Verma, H. Arora, W. Manalastas Jr., M. Srinivasan, ACS Appl. Energy Mater. 3 (2020) 8627–8635.
- [32] C. Yan, C. Lv, L. Wang, W. Cui, L. Zhang, K.N. Dinh, H. Tan, C. Wu, T. Wu, Y. Ren, J. Am. Chem. Soc. 142 (2020) 15295–15304.
- [33] W. Pan, Y. Wang, Y. Zhang, H.Y.H. Kwok, M. Wu, X. Zhao, D.Y. Leung, J. Mater. ChemA. 7 (2019) 17420–17425.
- [34] A.M. Zamarayeva, A.E. Ostfeld, M. Wang, J.K. Ducey, I. Deckman, B.P. Lechêne, G. Davies, D.A. Steingart, A.C. Arias, Sci. Adv. 3 (2017), e1602051.
- [35] P. Wang, Z. Chen, Z. Ji, Y. Feng, J. Wang, J. Liu, M. Hu, H. Wang, W. Gan, Y. Huang, Chem. Eng. J. 373 (2019) 580–586.
- [36] S. Liu, P. Wang, C. Liu, Y. Deng, S. Dou, Y. Liu, J. Xu, Y. Wang, W. Liu, W. Hu, Small 16 (2020) 2002856.
- [37] P. Wang, Z. Chen, H. Wang, Z. Ji, Y. Feng, J. Wang, J. Liu, M. Hu, J. Fei, W. Gan, Energy Stor. Mater. 25 (2020) 426–435.
- [38] T.H. Nguyen, A. Fraiwan, S. Choi, Biosens. Bioelectron. 54 (2014) 640–649.
- [39] D. Yuan, J. Zhao, W. Manalastas Jr., S. Kumar, M. Srinivasan, Nano Mater. Sci. (2019).
- [40] X. Cai, Y. Song, Z. Sun, D. Guo, X.-X. Liu, J. Power Sources 365 (2017) 126–133.
- [41] Y. Liu, M. Pharr, G.A. Salvatore, ACS Nano 11 (2017) 9614–9635.
- [42] A. Nag, S.C. Mukhopadhyay, J. Kosel, IEEE Sensor. J. 17 (2017) 3949–3960.
- [43] Y. Wang, H. Wang, J. Xuan, D.Y. Leung, Biosens. Bioelectron. (2020) 112410.
- [44] Y. Wang, H.Y. Kwok, W. Pan, Y. Zhang, H. Zhang, X. Lu, D.Y. Leung, Electrochim. Acta 319 (2019) 947–957.